

Pion pole light-by-light contribution to $g - 2$ of the muon in a nonlocal chiral quark model

Alexander E. Dorokhov*

Joint Institute for Nuclear Research, Bogoliubov Laboratory of Theoretical Physics, 141980, Moscow region, Dubna, Russia

Wojciech Broniowski†

*Henryk Niewodniczański Institute of Nuclear Physics,
Polish Academy of Sciences, PL-31342 Kraków, Poland; Institute of Physics,
Jan Kochanowski University, PL-25406 Kielce, Poland*

We calculate the pion pole term of the light-by-light contribution to the $g - 2$ of the muon in the framework of an effective chiral quark model with instanton-like nonlocal quark–quark interaction. The full kinematic dependence of the pion-photon transition form factors is taken into account. The dependence of form factors on the pion virtuality decreases the result by about 15% in comparison to the calculation where this dependence is neglected. Further, it is demonstrated that the QCD constraints suggested by Melnikov and Vainshtein are satisfied within the model. The corresponding contributions originate from the box diagram as well from the pion-pole term. Our chiral nonlocal model result for the pion-pole light-by-light contribution to $(g - 2)/2$ of the muon is $(6.3 - 6.7) \cdot 10^{-10}$, which is in the ball park of other effective-model calculations.

PACS numbers: 13.40.Em, 12.38.Lg, 14.40.Aq, 14.60.Ef

Keywords: muon gyromagnetic ratio, light-by-light scattering, instanton liquid, pion-photon transition form factor

I. INTRODUCTION

The E821 experiment at the Brookhaven National Laboratory has recently measured the anomalous magnetic moment of the muon, $a_\mu \equiv (g_\mu - 2)/2$, with the final result [1]:

$$a_\mu^{\text{exp}} = 11\,659\,208.0(6.3) \cdot 10^{-10}. \quad (1)$$

This unprecedented accuracy, with yet better precision expected in the planned experiments at BNL, JPARC, and FNAL [2], maintains the live interest in obtaining more accurate theoretical predictions for a_μ within the standard model, for reviews see, e.g., [3, 4, 5, 6]. The challenge is to obtain the theoretical uncertainty lower than the uncertainties for the nearest-future experiments, which will supply a powerful test for possible effects of contributions from the New Physics.

In the standard model the electromagnetic (QED), electroweak (EW), and hadronic (Had) effects contribute to a_μ . Taking into account the recent progress with the QED calculations and the latest result for a_e one obtains [7]

$$a_\mu^{\text{QED}} = 11\,658\,471.809(0.016) \cdot 10^{-10}. \quad (2)$$

The electroweak contribution to a_μ is also known accurately [8],

$$a_\mu^{\text{EW}} = 15.4(0.2) \cdot 10^{-10}. \quad (3)$$

The main source of the theoretical uncertainty is the hadronic contribution. There are three types of the leading hadronic contributions: the vacuum polarization, its next-to-leading folding with the QED and EW sectors, and the light-by-light (LbL) scattering process (Fig. 1). A recent phenomenological reanalysis of the contribution of the full hadron vacuum polarization insertion into the electromagnetic vertex of the muon [9] gives

$$a_\mu^{\text{Had,LO}} = 690.9(4.4) \cdot 10^{-10}. \quad (4)$$

*Electronic address: dorokhov@theor.jinr.ru

†Electronic address: Wojciech.Broniowski@ifj.edu.pl

The most recent estimate of the higher-order (HO) hadronic contributions performed in [10] provides the result

$$a_{\mu}^{\text{Had,HO}} = -9.8(0.1) \cdot 10^{-10}. \quad (5)$$

For the LbL contributions there are several model-dependent estimates:

$$a_{\mu}^{\text{Had,LbL}} = 8.3(3.2) \cdot 10^{-10} \quad [11, 12], \quad (6)$$

$$a_{\mu}^{\text{Had,LbL}} = 8.9(1.7) \cdot 10^{-10} \quad [13], \quad (7)$$

$$a_{\mu}^{\text{Had,LbL}} = 13.6(2.5) \cdot 10^{-10} \quad [14]. \quad (8)$$

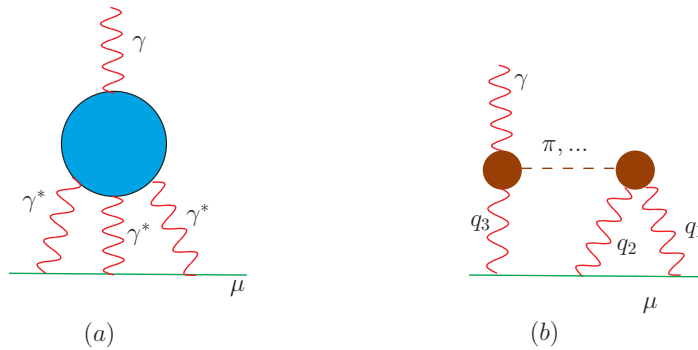


FIG. 1: (Color online) (a) Hadronic light-by-light contribution to a_{μ} . The bottom line is the muon, the wavy lines are the photons, and the circle depicts the hadronic part. (b) The meson pole contribution to a_{μ} . The circles represent the virtual meson to $\gamma^*\gamma^*$ transition form factors.

It is clear that the leading-order (LO) hadronic contribution (4) dominates in the absolute value. However, the theoretical error introduced by the LbL process (6)-(8) is of the same order as that for the leading term. Moreover, the error in (4) is phenomenologically well controlled and may be improved by a factor of 2 or so if more experimental data on $e^+e^-(\tau) \rightarrow \text{hadrons}$ should appear [9]. The precision for $a_{\mu}^{\text{Had,HO}}$ is quite enough for the nearest-future experiments. Unfortunately, the hadronic LbL contribution cannot be related to any other observable and hence we must rely on purely theoretical model framework in order to estimate it. Predictions based on chiral models (6), (7) (also in [15]) are compatible with one another and are much lower than the results obtained in (8) (also in [16, 17]). Furthermore, the errors given in (6)-(8) are difficult to estimate and it is not easy to improve their quality. These errors should include the model dependence, the dependence on model parameters, and the quality of the model assumptions. The last point, difficult to assess, is most important for our further discussion presented in this paper.

We digress that at present the calculation of the LbL contribution within lattice QCD is a quite difficult task [18], hence we cannot use lattices yet as a reliable source of information for the considered problem.

The present work is devoted to the calculation of the pion-pole contribution of the hadronic light-by-light scattering to a_{μ} within the nonlocal chiral quark model (N χ QM) [19, 20] motivated by the instanton model of the QCD vacuum [21, 22, 23]. In [20] the vector and axial-vector correlators were calculated and then these results were applied to compute the hadronic vacuum polarization contribution $a_{\mu}^{\text{Had,LO}}$ [24]. Later on the three-point PVV and VVA correlators were analyzed in [25, 26, 27] and the contribution of the $\gamma\gamma^*Z^*$ vertex to a_{μ} was estimated in [5]. The present calculation of the LbL contribution exhibits a few important improvements compared to the previous calculations in effective quark models. First of all, in the pion-pole contribution, which dominates the hadronic LbL part, we take into account the full kinematic dependence of the pion-photon form factors, including their dependence on the pion virtuality. The inclusion of this dependence diminishes the results for the contribution to a_{μ} by about 15% compared to the calculation with no dependence on the pion virtuality. Importantly, our approach is consistent with the low-energy theorems and with the QCD constraints. In particular, we demonstrate how the QCD constraint considered by Melnikov and Vainshtein [14] is satisfied at high photon momenta within N χ QM, with the crucial role of the box diagram. We also show that in general the pion-pole contribution exhibits no enhancement as it was assumed in the model [14] for the pion exchange in the LbL amplitude.

The next Section contains the definitions of the LbL amplitude, its pion-pole contribution, and the QCD constraint for the amplitude discussed in [14]. Sections III and IV describe the nonlocal chiral quark model based on instanton-like dynamics (N χ QM), introduces conserved vector and axial-vector currents, as well as the relevant PVV amplitude. This part, developed in previous works, is included for the completeness of the paper. Numerical results for the pion pole contribution to LbL and the comparison to other calculations are shown in Sections V and VI. In Section VII the Melnikov-Vainshtein constraint is proven within N χ QM. Conclusions are given in the last Section.

II. LIGHT-BY-LIGHT AMPLITUDE

The amplitude for the light-by-light scattering is defined as¹

$$\begin{aligned} \mathcal{M} &= \alpha^2 N_c \text{Tr} [\hat{Q}^4] \mathcal{A} = \alpha^2 N_c \text{Tr} [\hat{Q}^4] \mathcal{A}_{\mu_1 \mu_2 \mu_3 \gamma \delta} \epsilon_1^{\mu_1} \epsilon_2^{\mu_2} \epsilon_3^{\mu_3} f^{\gamma \delta} \\ &= -e^3 \int d^4 x d^4 y e^{-iq_1 x - iq_2 y} \epsilon_1^{\mu_1} \epsilon_2^{\mu_2} \epsilon_3^{\mu_3} \langle 0 | T \{ j_{\mu_1}(x) j_{\mu_2}(y) j_{\mu_3}(0) \} | \gamma \rangle, \end{aligned} \quad (9)$$

where q_i and ϵ_i are the momenta and the polarization vectors of photons, j_μ is the hadronic electromagnetic current defined explicitly below within the nonlocal chiral quark model, and \hat{Q} is the quark charge operator. The photon momenta are taken to be incoming, with $\sum q_i = 0$. One of the photons represents the external magnetic field and can be regarded as a real photon with a vanishingly small momentum, q_4 . Due to the gauge invariance the light-by-light scattering amplitude is proportional to the field strength tensor of the soft photon, $f^{\gamma \delta} = q_4^\gamma \epsilon_4^\delta - q_4^\delta \epsilon_4^\gamma$. Neglecting the quadratic and higher powers of q_4 , the tensor amplitude $\mathcal{A}_{\mu_1 \mu_2 \mu_3 \gamma \delta}$ may be considered as a function of the photon virtualities q_i^2 , $i = 1, 2, 3$ under the condition $q_1 + q_2 + q_3 = 0$.

In general the LbL amplitude is a rather complicated object to analyze. However, it is possible to generate different hierarchies for the components of the amplitude. The dominant contribution comes from the pole in the pseudoscalar channel, which is enhanced by the very small value of the pion mass (Fig. 1b). It is also leading in terms of the large- N_c counting, where N_c is the number of colors. Moreover, the leading- N_c contributions from other mesonic channels are suppressed by much larger meson masses.

It can be shown, see [12, 15, 28], that the leading contribution from the neutral pseudoscalar meson exchange to a_μ is given by

$$\begin{aligned} a_\mu^{\text{LbL}; \pi^0} &= -e^6 \int \frac{d^4 q_1}{(2\pi)^4} \int \frac{d^4 q_2}{(2\pi)^4} \frac{1}{q_1^2 q_2^2 q_3^2 [(p+q_1)^2 - m^2][(p-q_2)^2 - m^2]} \\ &\times \left[\mathcal{F}_{\pi_0^* \gamma^* \gamma^*}(q_2^2; q_1^2, q_3^2) \frac{G_P}{g_{\pi q}^2 (1 - G_P J_{pp}(q_2^2))} \mathcal{F}_{\pi_0^* \gamma^* \gamma^*}(q_2^2; q_2^2, 0) T_1(q_1, q_2; p) \right. \\ &\left. + \mathcal{F}_{\pi_0^* \gamma^* \gamma^*}(q_3^2; q_1^2, q_2^2) \frac{G_P}{g_{\pi q}^2 (1 - G_P J_{pp}(q_3^2))} \mathcal{F}_{\pi_0^* \gamma^* \gamma^*}(q_3^2; (q_1+q_2)^2, 0) T_2(q_1, q_2; p) \right], \end{aligned} \quad (10)$$

where m denotes the muon mass ($p^2 = m^2$) and the kinematic factors are [15]

$$\begin{aligned} T_1(q_1, q_2; p) &= \frac{16}{3} (p \cdot q_1) (p \cdot q_2) (q_1 \cdot q_2) - \frac{16}{3} (p \cdot q_2)^2 q_1^2 \\ &- \frac{8}{3} (p \cdot q_1) (q_1 \cdot q_2) q_2^2 + 8(p \cdot q_2) q_1^2 q_2^2 - \frac{16}{3} (p \cdot q_2) (q_1 \cdot q_2)^2 \\ &+ \frac{16}{3} m^2 q_1^2 q_2^2 - \frac{16}{3} m^2 (q_1 \cdot q_2)^2, \end{aligned} \quad (11)$$

$$\begin{aligned} T_2(q_1, q_2; p) &= \frac{16}{3} (p \cdot q_1) (p \cdot q_2) (q_1 \cdot q_2) - \frac{16}{3} (p \cdot q_1)^2 q_2^2 \\ &+ \frac{8}{3} (p \cdot q_1) (q_1 \cdot q_2) q_2^2 + \frac{8}{3} (p \cdot q_1) q_1^2 q_2^2 \\ &+ \frac{8}{3} m^2 q_1^2 q_2^2 - \frac{8}{3} m^2 (q_1 \cdot q_2)^2. \end{aligned} \quad (12)$$

The PVV amplitude $\mathcal{F}_{\pi_0^* \gamma^* \gamma^*}(q_3^2; q_1^2, q_2^2)$ for the virtual pion and photons, as well as the meson propagator in the pseudoscalar channel, $(1 - G_P J_{pp}(q_2^2))^{-1}$, will be discussed in Sect. IV.

Recently, an important constraint was introduced by Melnikov and Vainshtein (MV) [14], who argued with the help of the operator product expansion (OPE) that in the specific kinematic limit, $q_1^2 \approx q_2^2 \equiv q^2 \gg q_3^2$, the amplitude has the asymptotic form (see Fig. 2)

$$\mathcal{A}_{\mu_1 \mu_2 \mu_3 \gamma \delta} f^{\gamma \delta} = \frac{8}{\hat{q}^2} \epsilon_{\mu_1 \mu_2 \delta \rho} \hat{q}^\delta \sum_{a=3,8,0} W^{(a)} \left\{ w_L^{(a)}(q_3^2) q_3^\rho q_3^\sigma \tilde{f}_{\sigma \mu_3} + w_T^{(a)}(q_3^2) \left(-q_3^2 \tilde{f}_{\mu_3}^\rho + q_{3\mu_3} q_3^\sigma \tilde{f}_\sigma^\rho - q_3^\rho q_3^\sigma \tilde{f}_{\sigma \mu_3} \right) \right\} + \dots, \quad (13)$$

¹ In the following definitions we follow closely the notation used in [14].

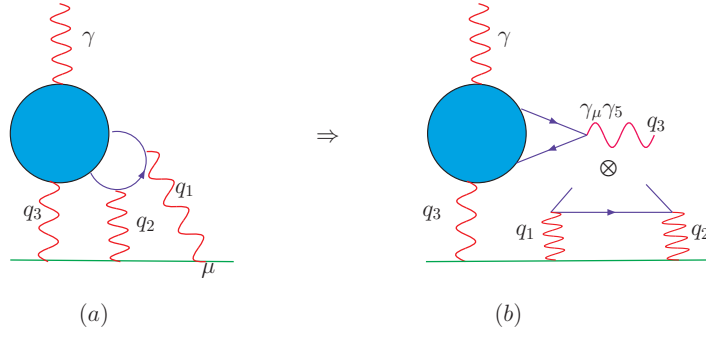


FIG. 2: (Color online) In the limit $q_1^2 \approx q_2^2 \gg q_3^2$ considered in [14] the LbL amplitude (a) factorizes in the leading twist into the VVA soft hadronic part and hard coefficient function, as indicated in (b).

where $\tilde{f}_{\alpha\beta} = \frac{1}{2}\varepsilon_{\alpha\beta\gamma\delta}f^{\gamma\delta}$, $\hat{q} = (q_1 - q_2)/2$ and no hierarchy between q_3^2 and Λ_{QCD}^2 is assumed. The weights $W^{(a)}$ are defined as

$$W^{(a)} = \frac{(\text{Tr}[\lambda_a \hat{Q}^2])^2}{\text{Tr}[\lambda_a^2] \text{Tr}[\hat{Q}^4]}; \quad (14)$$

$$W^{(3)} = \frac{1}{4}, \quad W^{(8)} = \frac{1}{12}, \quad W^{(0)} = \frac{2}{3}.$$

The invariant functions $w_L^{(a)}(q^2)$ and $w_T^{(a)}(q^2)$ are related to the triangle amplitude $T_{\gamma\rho}^{(a)}$ that involves the axial current $j_{5\rho}^{(a)}$ and two electromagnetic currents, one with momentum q and the other one (the external magnetic field) with the vanishing momentum (see the relevant part of Fig. 2b),

$$T_{\mu\rho}^{(a)} = i \langle 0 | \int d^4z e^{iqz} T \{ j_{5\rho}^{(a)}(z) j_\mu(0) \} | \gamma \rangle. \quad (15)$$

It is shown in [29] that $T_{\gamma\rho}^{(a)}$ can be written as

$$T_{\mu\rho}^{(a)} = -\frac{ie N_c \text{Tr}[\lambda_a \hat{Q}^2]}{4\pi^2} \left\{ w_L^{(a)}(q^2) q_\rho q^\sigma \tilde{f}_{\sigma\mu} + w_T^{(a)}(q^2) \left(-q^2 \tilde{f}_{\mu\rho} + q_\mu q^\sigma \tilde{f}_{\sigma\rho} - q_\sigma q^\sigma \tilde{f}_{\sigma\mu} \right) \right\}. \quad (16)$$

The first (second) amplitude is related to the longitudinal (transverse) part of the axial current, respectively. In the chiral limit w_L is fixed by the axial anomaly and the non-renormalization theorem predicts [29]

$$w_L^{(3,8)}(q^2) = 2/q^2. \quad (17)$$

In the hard limit $q^2 \gg \Lambda_{\text{QCD}}^2$ the perturbative QCD predicts the asymptotic form ($a = 3, 8, 0$)

$$w_T^{(a)}(q^2) = \frac{1}{2} w_L^{(a)}(q^2) = 1/q^2 \quad (18)$$

and (13) transforms into

$$\mathcal{A}_{\mu_1\mu_2\mu_3\gamma\delta} f^{\gamma\delta} = \frac{8}{q_3^2 \hat{q}^2} \varepsilon_{\mu_1\mu_2\delta\rho} \hat{q}^\delta \left\{ 2 q_3^\rho q_3^\sigma \tilde{f}_{\sigma\mu_3} + \left(-q_3^2 \tilde{f}_{\mu_3}^\rho + q_{3\mu_3} q_3^\sigma \tilde{f}_\sigma^\rho - q_3^\rho q_3^\sigma \tilde{f}_{\sigma\mu_3} \right) \right\} + \dots \quad (19)$$

It was demonstrated in [26, 27] that the results (16-18) are satisfied within the non-perturbative $N\chi\text{QM}$ approach.

In the next sections we discuss the basic elements of the $N\chi\text{QM}$. Then within this model we calculate the leading pion-pole contribution to a_μ , demonstrate how the Melnikov-Vainshtein asymptotics is realized, and finally discuss on the role of the triangle functions $w_{L(T)}$ for a_μ .

III. NON-LOCAL CHIRAL QUARK MODEL

To study the LbL contribution to a_μ one can use the framework of the effective field model of QCD. In the low-momenta domain the effects of the non-perturbative structure of the QCD vacuum become dominant. Since the invention of the QCD sum rule method based on the use of the standard OPE, it is common to parameterize the non-perturbative properties of the QCD vacuum in terms of infinite towers of the vacuum expectation values of the quark and gluon operators. From this point of view the nonlocal properties of the QCD vacuum result from the partial resummation of the infinite series of power corrections, related to vacuum averages of the quark and gluon operators of growing dimension, and may be parametrized in terms of the nonlocal vacuum condensates [30, 31, 32]. This construction leads effectively to nonlocal modifications of the propagators and effective vertices of the quark and gluon fields at small momenta.

An adequate model embodied in this general picture is the instanton model of the QCD vacuum [21, 22, 23] which describes non-perturbative nonlocal interactions in terms of the effective action (for a review see [33]). Spontaneous breaking of the chiral symmetry and the dynamical generation of a momentum-dependent quark mass are naturally explained within the instanton model. The non-singlet and singlet vector and axial-vector current-current correlators and the vector Adler function have been calculated in [20, 24] in the framework of the effective chiral model with instanton-like nonlocal quark-quark interaction [19, 20]. It was shown, in particular, that the Weinberg sum rules which are sensitive to the low- as well to the high-momentum dynamics are satisfied [20, 34]. In the same model the pion transition form factor normalized by the axial anomaly has been considered in [25] for arbitrary photon virtualities.

We start with the nonlocal chirally invariant action² which describes the interaction of soft quark fields [36],

$$\begin{aligned}
S = & \int d^4x \bar{q}_I(x) [i\gamma^\mu D_\mu - m_f] q_I(x) + \\
& + \frac{1}{2} G_P \int d^4X \int \prod_{n=1}^4 d^4x_n f(x_n) [\bar{Q}(X - x_1, X) \cdot \\
& \cdot \Gamma_P Q(X, X + x_3) \bar{Q}(X - x_2, X) \Gamma_P Q(X, X + x_4)],
\end{aligned} \tag{20}$$

where m_f is the current quark mass, $D_\mu = \partial_\mu - iV_\mu(x) - i\gamma_5 A_\mu(x)$ is the covariant derivative, and the matrix product $\Gamma_P \otimes \Gamma_P = (1 \otimes 1 + i\gamma_5 \tau^a \otimes i\gamma_5 \tau^a)$ provides the spin-flavor structure of the interaction. In Eq. (20) $\bar{q}_I = (\bar{u}, \bar{d})$ denotes the flavor doublet field of dynamically generated quarks, G_P is the four-quark coupling constant, and τ^a are the Pauli isospin matrices. The separable nonlocal kernel of the interaction described in terms of the form factors $f(x)$ is motivated by the instanton model of the QCD vacuum, where the function $f(x)$ may be evaluated. In order to make the nonlocal action gauge-invariant with respect to the external vector and axial gauge fields $V_\mu^a(x)$ and $A_\mu^a(x)$, we employ in (20) the delocalized quark field, $Q(x)$, defined with the help of the Schwinger gauge phase factors,

$$\begin{aligned}
Q(x, y) &= P \exp \left\{ i \int_x^y dz_\mu [V_\mu^a(z) + \gamma_5 A_\mu^a(z)] T^a \right\} q_I(y), \\
\bar{Q}(x, y) &= Q^\dagger(x, y) \gamma^0.
\end{aligned} \tag{21}$$

Here P stands for the operator ordering along the integration path, with y denoting the position of the quark and x being an arbitrary reference point.

The dressed quark propagator, $S(p)$, is found to be³

$$S^{-1}(p) = i\hat{p} - M(p^2), \tag{22}$$

with the momentum-dependent quark mass defined as the solution of the gap equation

$$M(p^2) = m_f + 4G_P N_f N_c f^2(p^2) \int \frac{d^4k}{(2\pi)^4} f^2(k^2) \frac{M(k^2)}{k^2 + M^2(k^2)}. \tag{23}$$

² In the present work we do not consider extensions of the model to include explicit vector mesons and the effects of the strange quark mass. Such extensions of the nonlocal model were considered in [24, 35] and will be used in *complete* calculations elsewhere.

³ From here on the Euclidean metric for the momenta is used.

The formal solution is expressed as [37]

$$M(p^2) = m_f + (M_q - m_f)f^2(p^2), \quad (24)$$

with the constant $M_q \equiv M(0)$ determined dynamically from Eq. (23). The momentum-dependent function $f(p)$ is the normalized four-dimensional Fourier transform of $f(x)$ given in the coordinate representation. Within the instanton model f is related to the zero mode solution for the massless fermion in the field of an instanton. In [26] it was shown that in the momentum space the nonlocal function $f(p)$ for large momenta must decrease faster than any inverse power of p^2 , *e.g.*, like an exponential, and that this choice corresponds to calculations in the axial gauge for the quark effective field. In order to take these effects into account and to make numerics simpler we use for the nonlocal function the Gaussian form,

$$f(p) = \exp(-p^2/\Lambda^2), \quad (25)$$

where the parameter Λ characterizes the nonlocality size of the gluon vacuum fluctuations and is proportional to the inverse average size of the instanton in the QCD vacuum.

An important property of the dynamical mass (23) is that at low virtualities its value is close to the constituent mass, while at large virtualities it goes to the current mass value. This property is crucial in obtaining the correct, consistent with the OPE, QCD behavior of different correlators at large momentum transfers [20, 24, 26]. The nonlocal chiral quark model can be viewed as an approximation to the large- N_c QCD, where the only (effective) interaction terms, retained after integrating out the high-frequency modes of the quark and gluon fields down to the nonlocality scale Λ where the spontaneous chiral symmetry breaking occurs, are those which can be cast in the form of the four-fermion operators (20). The parameters of the model are then the nonlocality scale Λ , the four-fermion coupling constant G_P , and the current quark masses m_f .

The quark-antiquark scattering matrix in the pseudoscalar channel is found from the Bethe-Salpeter equation as

$$\hat{T}_P(q^2) = \frac{G_P}{1 - G_P J_{PP}(q^2)}, \quad (26)$$

with the polarization operator in the pseudoscalar channel equal to

$$J_{PP}(q^2) = \int \frac{d^4k}{(2\pi)^4} f^2(k) f^2(k+q) \text{Tr} [S(k)\gamma_5 S(k+q)\gamma_5]. \quad (27)$$

The position of the pion state is determined as the pole of the scattering matrix

$$\det(1 - G_P J_{PP}(q^2)) \Big|_{q^2 = -m_\pi^2} = 0. \quad (28)$$

The quark-pion vertex identified with the residue of the scattering matrix is ($k' = k + q$)

$$\Gamma_\pi^a(k, k') = g_{\pi qq} i\gamma_5 \tau^a f(k) f(k') \quad (29)$$

with the quark-pion coupling equal to

$$g_{\pi q}^{-2} = - \left. \frac{dJ_{PP}(q^2)}{dq^2} \right|_{q^2 = -m_\pi^2}, \quad (30)$$

where m_π is the physical mass of the pion. In the chiral limit the quark-pion coupling, $g_{\pi q}$, and the pion decay constant, f_π , are connected by the Goldberger-Treiman relation, $g_\pi = M_q/f_\pi$, which is verified to be valid in N χ QM, as requested by the chiral symmetry.

IV. CONSERVED VECTOR AND AXIAL-VECTOR CURRENTS

The vector vertex following from the model (20) is

$$\Gamma_\mu(k, k') = \hat{Q} \left[\gamma_\mu + (k + k')_\mu M^{(1)}(k, k') \right], \quad (31)$$

where \hat{Q} is the diagonal matrix of the quark electric charges, $M^{(1)}(k, k')$ is the finite-difference derivative of the dynamical quark mass, k (k') is the incoming (outgoing) momentum of the quark, and $q = k' - k$ is the momentum corresponding to the current. The finite-difference derivative of an arbitrary function F is defined as

$$F^{(1)}(k, k') = \frac{F(k') - F(k)}{k'^2 - k^2}. \quad (32)$$

The full axial vertex corresponding to the conserved axial-vector current is obtained after the resummation of quark-loop chain that results in the form of the term proportional to the pion propagator [19]

$$\begin{aligned} \Gamma_\mu^{a,5}(k, k') &= [\gamma_\mu \gamma_5 + \Delta \Gamma_\mu^5(k, k')] \lambda_a, \\ \Delta \Gamma_\mu^5(k, k') &= 2\gamma_5 \frac{q_\mu}{q^2} f(k) f(k') \left[J_{AP}(0) - \frac{m_f G_P J_P(q^2)}{1 - G_P J_{PP}(q^2)} \right] + \gamma_5 (k + k')_\mu J_{AP}(0) \frac{(f(k') - f(k))^2}{k'^2 - k^2}, \end{aligned} \quad (33)$$

where we have introduced the notation

$$J_P(q^2) = \int \frac{d^4 k}{(2\pi)^4} f(k) f(k+q) \text{Tr} [S(k) \gamma_5 S(k+q) \gamma_5], \quad (34)$$

$$J_{AP}(q^2) = 4N_c N_f \int \frac{d^4 l}{(2\pi)^4} \frac{M(l)}{D(l)} \sqrt{M(l+q) M(l)}. \quad (35)$$

In the chiral limit of $m_f = 0$ one gets instead

$$\Delta \Gamma_\mu^5(k, k') = \gamma_5 \frac{q_\mu}{q^2} [M(k') + M(k)] + \gamma_5 \left[\frac{q_\mu}{q^2} - \frac{(k+k')_\mu}{k'^2 - k^2} \right] M_q (f(k') - f(k))^2. \quad (36)$$

The axial-vector vertex (33) has a pole at

$$q^2 = -m_\pi^2 = m_f \langle \bar{q}q \rangle / f_\pi^2 \quad (37)$$

where the Goldberger-Treiman relation and the definition of the quark condensate has been used. The pole is related to the denominator $1 - G_P J_{PP}(q^2)$ in Eq. (33), while q^2 in denominator is compensated by zero from the square bracket in the limit $q^2 \rightarrow 0$. This compensation follows from expansion of $J(q^2)$ functions near zero momentum

$$\begin{aligned} J_{PP}(q^2) &= G_P^{-1} - m_f \langle \bar{q}q \rangle M_q^{-2} - q^2 g_{\pi q}^{-2} + O(q^4), \\ J_{AP}(q^2 = 0) &= M_q, \quad J_P(q^2 = 0) = \langle \bar{q}q \rangle M_q^{-1}. \end{aligned} \quad (38)$$

It follows from this expansion that near pole position, $q^2 = -m_\pi^2$, one has for the factor in (10)

$$\frac{G_P}{g_{\pi q}^2 (1 - G_P J_{PP}(q_\pi^2))} = \frac{1}{q^2 + m_\pi^2} + \dots \quad (39)$$

However, at large q^2 this factor goes to the constant $G_P g_{\pi q}^{-2}$ instead of decay like q^{-2} as it would be predicted by the simple pole approximation. In the chiral limit $m_f = 0$ the second structure in square brackets in Eq. (33) disappears and the pole moves to zero. It should be stressed that the form of the interaction vertices (31,33) is consistent with the chiral Ward-Takahashi identities.

Within N χ QM the full singlet axial-vector vertex including local and nonlocal pieces is given by [20]

$$\begin{aligned} \Gamma_\mu^{0,5}(k, k') &= \gamma_\mu \gamma_5 + \Delta \Gamma_\mu^{0,5}(k, k'), \\ \Delta \Gamma_\mu^{0,5}(k, k') &= \gamma_5 \left[(k + k')_\mu M_q \frac{(f(k') - f(k))^2}{k'^2 - k^2} + \frac{q_\mu}{q^2} 2M_q f(k') f(k) \frac{G_P^0 (1 - G_P J_{PP}(q^2))}{G_P (1 - G_P^0 J_{PP}(q^2))} \right], \end{aligned} \quad (40)$$

where G_P^0 is the four-quark coupling for the singlet channel. As it follows from expansion (38) the singlet current (40) does not contain massless pole due to presence of the $U_A(1)$ anomaly. Instead, the singlet current develops a pole at the η' -meson mass

$$1 - G_P^0 J_{PP}(q^2 = -m_{\eta'}^2) = 0, \quad (41)$$

thus solving the $U_A(1)$ problem.

The parameters of the model are fixed in a way typical for effective low-energy quark models. One usually fits the pion decay constant, f_π , and the pion mass (28) to their experimental values. In the chiral limit the decay constant reduces to $f_{0,\pi} = 86$ MeV [38]. In $N\chi$ QM $f_{0,\pi}$ is expressed as [23]

$$f_{0,\pi}^2 = \frac{N_c}{4\pi^2} \int_0^\infty dk^2 k^2 \frac{M^2(k^2) - k^2 M(k^2) M'(k^2) + k^4 M'(k^2)^2}{(k^2 + M^2(k^2))^2}, \quad (42)$$

where the primes mean the derivatives with respect to k^2 , *i.e.* $M'(k^2) = dM(k^2)/dk^2$, *etc.* The described fitting procedure introduces two relations among the three model parameters. We use the following values of the model parameters fixed in Ref. [24]:

$$M_q = 0.24 \text{ GeV}, \quad \Lambda_P = 1.11 \text{ GeV}, \quad m_f = 8 \text{ MeV}. \quad (43)$$

To test the sensitivity of the results on the choice of parameters we also use the set [25]

$$M_q = 0.35 \text{ GeV}, \quad \Lambda_P = 1.2 \text{ GeV}, \quad m_f = 12 \text{ MeV}. \quad (44)$$

Both sets reproduce the low-energy observables with an acceptable accuracy of the order of 10%. The finite current quark mass in (43) and (44) is fixed by the physical value of pion mass. It also increases the pion decay constant to its experimental value, $f_\pi = 92$ MeV, within a 2 MeV accuracy.

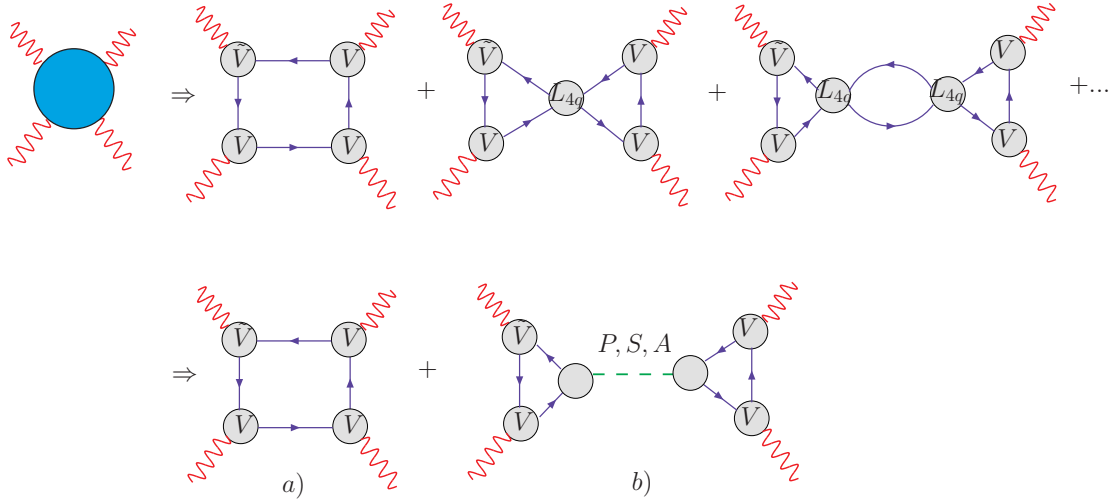


FIG. 3: (Color online) The diagrammatic representation of the LbL scattering amplitude within the effective four-quark model in the leading $1/N_c$ approximation. It consists of the box diagram plus the iteration of the four-quark interaction term via the quark loop. The iterative terms sum up into a two-point meson correlator in the given channel (pseudoscalar, scalar, or axial-vector). All quark lines and the vertices are dressed, as calculated within $N\chi$ QM. There are also a number of contact terms inherent to nonlocal models, not shown in the figure.

The triangle PVV amplitude corresponding to the process $\gamma^* \gamma^* \rightarrow \pi_0^*$

$$A(\gamma^*(q_1, \epsilon_1) \gamma^*(q_2, \epsilon_2) \rightarrow \pi_0^*(p)) = -ie^2 \epsilon_{\mu\nu\rho\sigma} \epsilon_1^\mu \epsilon_2^\nu q_1^\rho q_2^\sigma \mathcal{F}_{\pi_0^* \gamma^* \gamma^*}(q_3^2; q_1^2, q_2^2), \quad (45)$$

has been constructed and discussed in [25]⁴. In (45) ϵ_i^μ and q_i ($i = 1, 2$) are the photon polarization vectors and momenta, while $q_3 = q_1 + q_2$ is the pion momentum. In $N\chi$ QM one finds the contribution of the triangle diagram to the invariant amplitude as

$$A(\gamma_1^* \gamma_2^* \rightarrow \pi_0^*) = -ie^2 \frac{N_c}{f_\pi} \text{Tr}[\widehat{Q}^2 \tau^3] \epsilon_1^\mu \epsilon_2^\nu \int \frac{d^4 k}{(2\pi)^4} \text{Tr}[\Gamma_\pi^a(k_+, k_-) S(k_-) \Gamma_\mu(k_-, k_3) S(k_3) \Gamma_\nu(k_3, k_+) S(k_+)] \quad (46) \\ + (q_1 \leftrightarrow q_2; \epsilon_1 \leftrightarrow \epsilon_2).$$

⁴ In [25] the amplitude $\mathcal{F}_{\pi_0^* \gamma^* \gamma^*}$ is denoted as M_{π_0} .

where $q = q_1 - q_2$, $k_{\pm} = k \pm q_3/2$, $k_3 = k - q/2$. In the chiral limit ($q_3^2 = m_{\pi}^2 = 0$) with both photons real ($q_i^2 = 0$) one finds the normalization by the axial anomaly (within the nonlocal models it was proven in [35])

$$\mathcal{F}_{\pi_0^* \gamma^* \gamma^*}(0; 0, 0) = \frac{N_c}{12\pi^2 f_{\pi}}. \quad (47)$$

The functions defined in (26), (27), (45), (46) are used in the evaluation of (10). Within the effective model the light-by-light amplitude is given by diagrams of Fig. 3.

V. NUMERICAL RESULTS FOR THE PION POLE CONTRIBUTION TO LbL

We first investigate the role of the off-shellness in the pion transition form factor $\mathcal{F}_{\pi_0^* \gamma^* \gamma^*}(q_3^2; q_1^2, q_2^2)$, which is the important element considered in this work. In Fig. 4 we show how $\mathcal{F}_{\pi_0^* \gamma^* \gamma^*}(q_3^2; q_1^2, q_2^2)/\mathcal{F}_{\pi_0^* \gamma^* \gamma^*}(0; 0, 0)$ depends on q_3 for fixed values of q_1 and q_2 . For all cases of q_1 and q_2 we note a strong dependence on q_3 , which for large values of this momentum becomes exponential, $\sim \exp(-\text{const} \cdot q_3^2)$. This strong dependence on the off-shellness, related to the Gaussian form of the nonlocal quark-pion vertex (29), could in principle lead to a significant reduction of the pion pole contribution to LbL. As we shall see below, this is not the case, since the effective support for the integrand of $a_{\mu}^{\text{LbL}, \pi_0}$ is localized at moderate values of q_3^2 where the form factor suppression is not so strong. Furthermore, the factor $(1 - G_P J_{pp}(q_3^2))^{-1}$ in Eq. (10) at large q_3^2 goes to one, but not to q_3^{-2} as in the case of the single-pole approximation $(q_3^2 - m_{\pi}^2)^{-1}$.

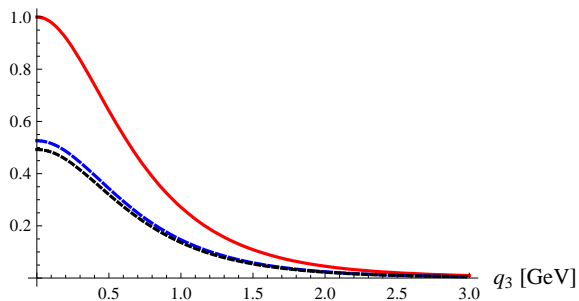


FIG. 4: (Color online) The dependence of the pion transition form factor $\mathcal{F}_{\pi_0^* \gamma^* \gamma^*}(q_3^2; q_1^2, q_2^2)/\mathcal{F}_{\pi_0^* \gamma^* \gamma^*}(0; 0, 0)$ on the off-shellness of the pion, $|q_3|$, for $q_1^2 = q_2^2 = 0$ (top curve), $q_1^2 = (700 \text{ MeV})^2$, $q_2^2 = 0$ (middle curve), and for $q_1^2 = q_2^2 = (700 \text{ MeV})^2/2$ (bottom curve). We note a strong dependence on $|q_3|$ (all momenta are Euclidean).

To obtain $a_{\mu}^{\text{LbL}, \pi_0}$, one has to convolute the three-point vertex functions discussed above in the two-loop integral of Eq. (10). Since the multidimensional integrand is a regular function, this task can be accomplished straightforwardly with the Monte Carlo integration technique. We use the routine VEGAS [39], which implements the adaptive Monte Carlo algorithm. The eight-dimensional⁵ integral in (10), carried over the the two muon loop momenta, has been done numerically in the Euclidean space.

A convenient and important trick, allowing to avoid the numerical cut-offs in the momentum integration, is to map the momentum variables via a conformal transformation into the range $[0, 1)$. Explicitly, we use

$$\xi_i = \frac{p_i^2}{p_i^2 + a}, \quad (48)$$

with p_i denoting the Euclidean momentum and $a = 1 \text{ GeV}^2$. We have tested the accuracy of our code by reproducing very accurately various model results listed in Ref. [15].

The result of the calculation in N χ QM with parameters (43) is

$$a_{\mu}^{\text{LbL}, \pi_0} = 6.27 \cdot 10^{-10}. \quad (49)$$

⁵ Through the use of the rotational symmetry one may reduce the integral down to five dimensions, but from the view point of the Monte Carlo integration this is irrelevant for the performance.

while with parameters (44) we get

$$a_\mu^{\text{LbL},\pi_0} = 6.68 \cdot 10^{-10}. \quad (50)$$

Similarly to other models, our result is dominated by the term proportional to the T_1 structure in Eq. (10), which yields 97% of the total of (49,50).

In order to illustrate the convergence of the result with the increasing upper limit of the momentum integration, here denoted by Λ , we show in Fig. 5 the relative yield of the full result for a_μ^{LbL,π_0} with model parameters (44), plotted as a function of the Euclidean momentum cut-off, Λ ($|p_i| \leq \Lambda$). For $\Lambda \rightarrow \infty$ we obtain, by definition, the full result. For $\Lambda = 1$ GeV about 90% of the full result is obtained. Thus the result is dominated by the soft physics, as requested of the effective low-energy model. These findings are in agreement with that obtained in [15, 40].

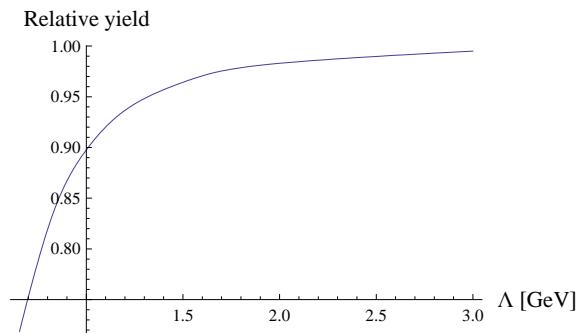


FIG. 5: (Color online) The relative yield of the full result for a_μ^{LbL,π_0} for model parameters (44), plotted as a function of the Euclidean momentum cut-off, Λ .

Finally, we note that in the extended version of the considered model the vector and axial-vector couplings appear. However, as it was discussed in [25] within the nonlocal model, the inclusion of these couplings leads to very minor changes of the pion transition form factor. In particular, it does not change the normalization of the form factor at zero momentum and contributes small corrections to the leading-order asymptotics. The latter is due to the relatively large mass of the rho meson.

VI. COMPARISON TO OTHER APPROACHES

In this section we compare our calculation of the pion-pole light-by-light contribution to a_μ with the results obtained in earlier calculations [11, 13, 15]

$$a_\mu^{\pi^0, \text{LbL}} = 5.6 \cdot 10^{-10} \quad [11], \quad (51)$$

$$a_\mu^{\pi^0, \text{LbL}} = 5.6 \cdot 10^{-10} \quad [13], \quad (52)$$

$$a_\mu^{\pi^0, \text{LbL}} = 5.8(1.0) \cdot 10^{-10} \quad [15]. \quad (53)$$

These calculations are based on the usage of different parameterizations of the $\pi\gamma^*\gamma^*$ vertex satisfying the CLEO data on the pion transition form factor $\pi \rightarrow \gamma\gamma^*$ and OPE constraints. Thus, in [15] the phenomenological form factor from the generalized vector-meson dominance (VMD) was used (the Knecht-Nyffeler (KN) model),

$$F_{\pi\gamma^*\gamma^*}^{\text{gVMD}}(s, t) = \frac{f_\pi (s+t)st - h_2st + h_5(s+t) + M_V^4 M_{V_1}^4 h_7}{3 (M_V^2 + s)(M_V^2 + t)(M_{V_1}^2 + s)(M_{V_1}^2 + t)}, \quad (54)$$

with the parameters $M_V = 769$ MeV, $M_{V_1} = 1465$ MeV, $h_5 = 6.93$ GeV⁴, $h_7 = N_c/(4\pi^2 f_\pi^2)$. The error in (53) is due to the uncertainty of the parameter h_2 taken from the interval $h_2 \in [10, -10]$ GeV². However, the function (54) depends on two kinematic variables instead of three required by (10). We test the effect of this approximation. Namely, in (46) we have removed the dependence on the pion virtuality and have taken the meson propagator in (10) in the single-pole approximation $1/(p^2 - m_\pi^2)$. In the N χ QM we obtain numerically for the parameter set (43)

$$a_\mu^{\text{LbL},\pi_0} = 7.33 \cdot 10^{-10} \quad (\text{no off-shellness effects}). \quad (55)$$

This result should be compared to the full calculation yielding (49). Thus, as already stated, the inclusion of the dependence on the pion virtuality reduces the result by about 15%. A similar statement that the influence of the pion off-shellness has only a small effect was presented in [15]. In that work different form factors, including the point-like pion coupling and the form factors used in the extended Nambu–Jona-Lasinio (ENJL) model of [11, 12], were tested. The stability of the results was demonstrated.

Recently, there was an attempt by Jegerlehner and Nyffeler [41] to improve the KN model by taking into account the full kinematic dependence of the pion-photon vertex through the use of the parametrization for $F_{\pi^* \gamma^* \gamma^*}^{\text{gVMD}}(s, t, u)$ suggested in [42]. This yields for the sum of the π, η, η' contributions $a_\mu^{\text{LbL}, \pi_0, \eta, \eta'} = 9.66 \pm 4.5 \cdot 10^{-10}$. As a result an enhancement of the contribution in comparison with KN result $a_\mu^{\text{LbL}, \pi_0, \eta, \eta'} = 8.3 \pm 1.2 \cdot 10^{-10}$ was obtained. We believe that this is a result of neglecting the dressing effects in the parametrization constructed in [42]. In particular, this parametrization reproduces the short-distance behavior of the three-point correlator of the pseudoscalar and vector currents [42]. For these currents the local γ_5 and γ_μ couplings were used, correspondingly. Because of the local character of these vertices the correlator has a slow power-like behaviour at large momenta. However, this correlator does not correspond to the triangle quark diagram connecting the virtual pion with the photons. The pion has its own hadronic form factor, which means that the γ_5 vertex is dressed, as it corresponds to the nonlocal form factor (29) (see the similar results in the Schwinger-Dyson approach [43]). As a result the large-momentum properties of the calculation change drastically.

Similar problems are encountered in calculations based on the usage of the constant constituent quark mass (the local models) [16, 17]. Typically, these models predict larger numbers for the hadronic contribution due to incorrect form factors, artificially enhanced with respect to the OPE asymptotics.

We have to note that our approach is closest to the formalism of the work [12] (ENJL model) in the sense of the use of techniques of the effective models. However, the physical grounds are quite different. The ENJL model is in fact a generalization of the vector meson dominance model, while $N\chi\text{QM}$ is based on the fundamental property of the QCD vacuum, namely the nonlocality of the vacuum fluctuations of the gluon field. Unfortunately, the region of applicability of the ENJL model is restricted to momenta much lower than 1 GeV. For example, we are not able to prove the properties of the triangle diagram (16-18) by using the VVA functions found in the ENJL model [12]. The inconsistency of the Adler function found within ENJL with the OPE was noted earlier in [24]. The high-momentum region was then modeled in [12] by different parameterizations, which may be quite risky. One of us (AD) has already pointed out in [24] that a possible reason for the failure of ENJL at large momenta is due to the fact that this model is based on the single resonance approximation, while nonlocalities, inherent in $N\chi\text{QM}$, effectively take into account an infinite number of resonances according to the quark-hadron duality principle. One of the results that is observed in [12] is that there are large cancellations of different contributions. This might be a model-dependent statement that has to be checked in future *complete* calculations within the nonlocal chiral quark model with instanton-like interactions.

VII. THE MELNIKOV-VAINSHTEIN CONSTRAINT IN $N\chi\text{QM}$

The sole contribution of the pion pole discussed in the previous sections and also used in [11] and [15] does not satisfy the Melnikov-Vainshtein (MV) asymptotics (19) discussed in Sect. II. In the present section we show within the $N\chi\text{QM}$ model that it is the quark box diagram of the light-by-light scattering that provides the correct asymptotics (Fig. 3a). To this end we first recall the properties of the non-diagonal correlator of the vector current and the axial-vector current in the external electromagnetic field ($V\tilde{A}\tilde{V}$) (15), as derived in [26, 27] within $N\chi\text{QM}$. In this model the $V\tilde{A}\tilde{V}$ correlator is defined by (Fig. 6)

$$T_{\mu_3\rho}^a = -2eN_c \text{Tr} \left[\tilde{Q}^2 \lambda^a \right] \epsilon_4^\nu \int \frac{d^4k}{(2\pi)^4} \text{Tr} \left[\Gamma_{\mu_3}(k+q_3, k) S(k+q_3) \cdot \right. \\ \left. \cdot \Gamma_{\rho}^{a,5}(k+q_3, k-q_4) S(k-q_4) \tilde{\Gamma}_\nu(k, k-q_4) S(k) \right], \quad (56)$$

where for definiteness we consider q_4 as a soft momentum. The quark propagator, the vector vertex, and the nonsinglet and singlet axial-vector vertices are given in (22), (31), (33), and (40), respectively. The structure of the vector vertices guarantees that the amplitude is transverse with respect to the vector indices

$$T_{\mu_3\rho}^a q_3^{\mu_3} = 0, \quad (57)$$

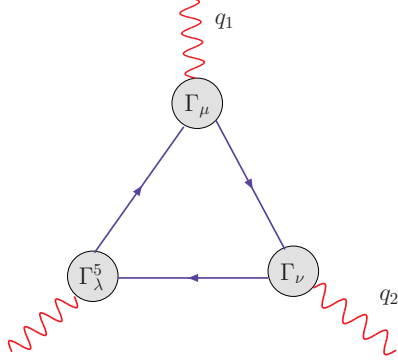


FIG. 6: (Color online) Diagrammatic representation of the triangle diagram in the instanton model with dressed quark lines and full quark-current vertices

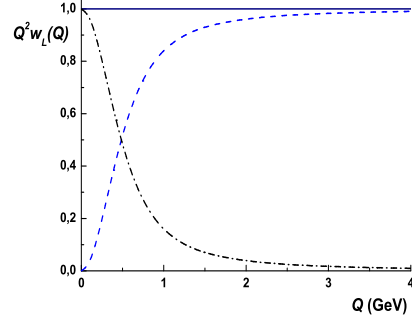


FIG. 7: (Color online) The normalized nonsinglet invariant function w_L constrained by the Adler-Bell-Jackiw anomaly following from the triangle diagram. The dashed line denotes the local part and the dash-dotted line the nonlocal part.

while the Lorentz structure of the amplitude is given by (16). It is convenient to separate the correlator into three pieces:

$$T_{\mu_3\rho}^{a,Loc} = -2eN_c Tr \left[\widehat{Q}^2 \lambda^a \right] \epsilon_4^\nu \int \frac{d^4 k}{(2\pi)^4} Tr \left[\gamma_{\mu_3} S(k+q_3) \gamma_\rho \gamma_5 S(k-q_4) \gamma_\nu S(k) \right], \quad (58)$$

$$T_{\mu_3\rho}^{a,Pole} = -2eN_c Tr \left[\widehat{Q}^2 \lambda^a \right] \epsilon_4^\nu \int \frac{d^4 k}{(2\pi)^4} Tr \left[\Gamma_{\mu_3}(k+q_3, k) S(k+q_3) \Delta \Gamma_\rho^5(k+q_3, k-q_4) S(k-q_4) \tilde{\Gamma}_\nu(k, k-q_4) S(k) \right], \quad (59)$$

$$T_{\mu_3\rho}^{a,Rest} = T_{\mu_3\rho}^a - T_{\mu_3\rho}^{a,Loc} - T_{\mu_3\rho}^{a,Pole}. \quad (60)$$

In Fig. 7 it is shown (for details see [26]) how the different terms saturate the anomalous nonsinglet amplitude w_L (17). The part $T_{\mu_3\rho}^{a,Loc}$, where all vertices are local, saturates the anomaly at large momenta, which is just the property of the quark triangle diagram (dashed line in Fig. 7)

$$T_{\mu_3\rho}^{a,Loc} \Big|_{\substack{q_4 \text{ soft} \\ q_3 \gg 1 \text{ GeV}}} \rightarrow T_{\mu_3\rho}^a. \quad (61)$$

This result (61) is independent of the channel and the relations (18) become true (see [26, 27] for details).

It is the pole term (59) which dominates the low-momentum behavior of the amplitude sensitive to the flavor structure of the axial current. In the nonsinglet channel at zero momentum the anomaly is saturated by the massless pion pole contribution (59) (dash-dotted line in Fig. 7). The remaining part $T_{\mu_3\rho}^{a,Rest}$, which vanishes at zero and infinite momenta and is numerically small everywhere, accomplishes the exact saturation to the correct value at all momenta. On the other hand, in the singlet case due to different structure of the singlet current (40) the pole contribution (59) is almost completely compensated and the local part (58) dominates the amplitude at all momenta [27].

With this background in mind let us now consider the LbL scattering amplitude coming from the box diagram with dynamical quarks (q_4 is a soft momentum)

$$\begin{aligned} \mathcal{A}_{\mu_1\mu_2\mu_3\gamma\delta}^{Box} f^{\gamma\delta} &= \epsilon_4^{\mu_4} \int \frac{d^4 k}{\pi^2} Tr \left[S(k) \Gamma_{\mu_4}(k, k+q_4) S(k+q_4) \Gamma_{\mu_1}(k+q_4, k+q_4+q_1) S(k+q_4+q_1) \right. \\ &\quad \left. \Gamma_{\mu_2}(k+q_4+q_1, k-q_3) S(k-q_3) \Gamma_{\mu_3}(k-q_3, k) \right]. \end{aligned} \quad (62)$$

The kinematic limit considered by Melnikov and Vainshtein ($q_1^2 \approx q_2^2 \equiv q^2 \gg q_3^2$) is very similar to the case of the pion transition form factor with highly virtual photons analyzed within N χ QM in [25, 44]. In this limit one has

$$\mathcal{A}_{\mu_1\mu_2\mu_3\gamma\delta}^{Box} f^{\gamma\delta} = -\frac{2\pi^2 i}{\widehat{q}^2} \varepsilon_{\mu_1\mu_2\delta\rho} \widehat{q}^\delta \epsilon_4^{\mu_4} \int \frac{d^4 k}{\pi^2} Tr \left[S(k) \Gamma_{\mu_4}(k, k+q_4) S(k+q_4) \gamma_\rho \gamma_5 S(k-q_3) \Gamma_{\mu_3}(k-q_3, k) \right] + \dots, \quad (63)$$

where the higher power corrections are denoted by dots. The result (63) is proportional to the correlator $T_{\mu_3\rho}^{a,\text{Loc}}$ which, as discussed above, saturates the full triangle amplitude at $q_3^2 \gg 1 \text{ GeV}^2$. Thus, within N χ QM it is the box diagram which saturates the MV large- \hat{q}^2 asymptotics (19) at $q_3^2 \gg 1 \text{ GeV}^2 \approx \Lambda_{\text{QCD}}^2$. At the same time at $q_3^2 \ll 1 \text{ GeV}^2$ the box diagram contribution to the asymptotics is suppressed as it is seen from the behavior of the dashed line in Fig. 7.

In the regime $q_3^2 \ll 1 \text{ GeV}^2$ the MV asymptotics arises due to the pion-pole diagram discussed above (Fig. 3b). Indeed, we have

$$\begin{aligned} \mathcal{A}_{\mu_1\mu_2\mu_3\gamma\delta}^{\pi\text{-Pole}} f^{\gamma\delta} &= \left(\frac{\text{Tr} [\hat{Q}^2 \lambda_a]}{\text{Tr} [\hat{Q}^4]} \right)^2 \frac{G_P}{1 - G_P J_{PP}(q_3 + q_4)} \\ &\epsilon_4^{\mu_4} \int \frac{d^4 p}{(2\pi)^4} f(p - q_3) f(p + q_4) \text{Tr} [\Gamma_{\mu_4} S(p + q_4) i\gamma_5 S(p - q_3) \Gamma_{\mu_3} S(p)] \\ &N_c \int \frac{d^4 k}{(2\pi)^4} f(k - q_1) f(k + q_2) \text{Tr} [i\gamma_5 S(k - q_1) \Gamma_{\mu_1} S(k) \Gamma_{\mu_2} S(k + q_2)]. \end{aligned} \quad (64)$$

The MV limit taken for the second integral corresponds to the asymptotics of the transition form factor for the pion of fixed virtuality considered earlier in [25, 44]

$$\begin{aligned} &N_c \int \frac{d^4 k}{(2\pi)^4} f(k - q_1) f(k + q_2) \text{Tr} [i\gamma_5 S(k - q_1) \Gamma_{\mu_1} S(k) \Gamma_{\mu_2} S(k + q_2)] \\ &= \frac{2i}{\hat{q}^2} \varepsilon_{\nu\lambda\delta\sigma} \hat{q}^\delta N_c \int \frac{d^4 k}{(2\pi)^4} f(k - q_1) f(k + q_2) \text{Tr} [S(k - q_1) i\gamma_5 S(k + q_2) \gamma_\sigma \gamma_5] + \dots \\ &= \frac{2i}{\hat{q}^2} \varepsilon_{\nu\lambda\delta\sigma} \hat{q}^\delta q_3^\sigma \frac{f_\pi(q_3)}{\text{Tr} [\lambda_a^2]} + \dots \end{aligned} \quad (65)$$

Thus the asymptotics of the LbL pion-pole diagram in the MV limit is

$$\mathcal{A}_{\mu_1\mu_2\mu_3\gamma\delta}^{\pi\text{-Pole}} f^{\gamma\delta} = \frac{2i}{\hat{q}^2} \varepsilon_{\mu_1\mu_2\delta\rho} \hat{q}^\delta W^{(a)} \Delta T_{\mu_3\rho} + \dots \quad (66)$$

where

$$\Delta T_{\mu_3\rho}(q_3, q_4) = q_3^\lambda f_\pi(q_3^2) N_c \int \frac{d^4 p}{(2\pi)^4} \text{Tr} [\Gamma_{\mu_3} S(p + q_4) i\gamma_5 S(p - q_3) \Gamma_\rho S(p)] \frac{G_P f(p - q_3) f(p + q_4)}{1 - G_P J_{PP}(q_3)}. \quad (67)$$

This expression is similar to $T_{\mu_3\rho}^{\text{Pole}}$ in (59). If the renormalization of the axial vertex in (67) coincided with $\Delta\Gamma_\mu^5(k, k')$ in (33) then combining (63) and (66) one would reproduce the MV asymptotics (13) for all values of q_3^2 . However, the factor $f_\pi(q_3)$ has a strong dependence on the pion virtuality q_3^2 and thus the required $1/q_3^2$ dependence of the amplitude appears only from the pion-pole factor in (67) at $q_3^2 \ll 1 \text{ GeV}^2$.

The conclusions of this Section are: 1) We exactly reproduce the MV asymptotics (19) in the regime $q_3^2 \gg 1 \text{ GeV}$ from the quark box contribution to the LbL amplitude. 2) In the low-momentum region where effects of the infrared dynamics may be important we show how this asymptotics arises from the pion-pole triangle diagram near the position of the pole. 3) It might be possible that the MV asymptotics for arbitrary values of q_3^2 is reproduced within N χ QM if we consider the contact terms contributing to the four-point amplitude, neglected in the present study. 4) It follows from the above results that we partially agree with MV when these authors state that the ‘‘pion-pole’’ contribution considered in [14] is an attempt to describe the *complete*, on- and off-shell light-by-light scattering amplitude in the pseudoscalar isotriplet channel. 5) However, the N χ QM model calculations do not support the factorization ansatz (10), with one form factor replaced by a constant, used by MV in order to simulate this *complete* amplitude⁶. 6) Finally, we agree with [40] that in the MV model numerically one obtains $a_{\mu,MV}^{\pi^0,\text{LbL}} = 7.97 \cdot 10^{-10}$ instead of $7.65 \cdot 10^{-10}$ quoted

⁶ Moreover, the MV model does not fit the amplitude in other asymptotic perturbative QCD regimes: $q_1^2 \sim q_2^2 \sim q_3^2 \gg \Lambda_{\text{QCD}}^2$ and $q_1^2 \sim q_3^2 \gg q_2^2 \gg \Lambda_{\text{QCD}}^2$. In N χ QM when the photon virtualities are large the effective quark propagator connecting the hard photon vertices (γ_μ) becomes the usual massless quark propagator. Thus, the asymptotics of the quark box diagram (Fig. 3a) is the same as in N χ QM as well as in perturbative QCD for the massless quark considered in [14]. In the ENJL model the quark box diagram is suppressed at large photon virtualities by additional VMD form factors.

originally in [14]. Presumably, the discrepancy has its origin in the numerical treatment of the large-momentum tails in the integrals. With the conformal variables, we treat these tails exactly.

While the inclusion of the box diagram is crucial for the consistency of the N χ QM, the numerical evaluation of its contribution to LbL is beyond the scope of this paper. We remark, that in the ENJL model [12] the result is $2.1(0.3) \cdot 10^{-10}$, hence is a few times smaller than the dominant pion pole term.

VIII. CONCLUSIONS

In this paper we have analyzed the leading pion-pole contribution to $a_{\mu}^{\pi^0, \text{LbL}}$ in the nonlocal chiral quark model. The basic new element of our work is the inclusion of the full kinematic dependence of the pion-photon transition form factors, as it follows from the nonlocal chiral quark model. The dependence of the form factors on the pion virtuality decreases the result by about 15% compared to the case where this dependence is neglected. We have also demonstrated that the Melnikov-Vainshtein constraints, necessary for the consistency of the approach with QCD, are satisfied within the model when the quark box diagram is incorporated. Numerically, we quantitatively confirm the results obtained in other effective quark models.

An important next step in the investigations of the light-by-light scattering within nonlocal quark model is to perform an extension to the so-called *complete* calculation (see [12, 13, 16]), which includes the scalar, axial-vector, and the η, η' meson exchanges, as well as takes into account the quark and meson box diagrams. Due to contact terms arising in the nonlocal model, such a calculation is technically rather involved and will be presented elsewhere.

IX. ACKNOWLEDGMENTS

We thank S. Eidelman, F. Jegerlehner, N. I. Kochelev, E. A. Kuraev for their interest in this work. AD thanks for the partial support from Scient. School grant 195.2008.2 and the JINR Bogoliubov–Infeld program. WB thanks for the support from the Polish Ministry of Science and Higher Education, grants N202 034 32/0918 and N N202 249235.

-
- [1] G. W. Bennett *et al.* (Muon (g-2) Collaboration), Phys. Rev. **D73**, 072003 (2006), hep-ex/0602035.
 - [2] D. W. Hertzog, J. P. Miller, E. de Rafael, B. Lee Roberts, and D. Stockinger, (2007), 0705.4617.
 - [3] J. P. Miller, E. de Rafael, and B. L. Roberts, Rept. Prog. Phys. **70**, 795 (2007), hep-ph/0703049.
 - [4] M. Passera, Nucl. Phys. Proc. Suppl. **169**, 213 (2007), hep-ph/0702027.
 - [5] A. E. Dorokhov, Acta Phys. Polon. **B36**, 3751 (2005), hep-ph/0510297.
 - [6] F. Jegerlehner, Acta Phys. Polon. **B38**, 3021 (2007), hep-ph/0703125.
 - [7] M. Passera, Phys. Rev. **D75**, 013002 (2007), hep-ph/0606174.
 - [8] A. Czarnecki, W. J. Marciano, and A. Vainshtein, Phys. Rev. **D67**, 073006 (2003), hep-ph/0212229.
 - [9] S. Eidelman, Acta Phys. Polon. **B38**, 3015 (2007).
 - [10] K. Hagiwara, A. D. Martin, D. Nomura, and T. Teubner, Phys. Rev. **D69**, 093003 (2004), hep-ph/0312250.
 - [11] J. Bijnens, E. Pallante, and J. Prades, Nucl. Phys. **B626**, 410 (2002), hep-ph/0112255.
 - [12] J. Bijnens, E. Pallante, and J. Prades, Nucl. Phys. **B474**, 379 (1996), hep-ph/9511388.
 - [13] M. Hayakawa and T. Kinoshita, Phys. Rev. **D57**, 465 (1998), hep-ph/9708227.
 - [14] K. Melnikov and A. Vainshtein, Phys. Rev. **D70**, 113006 (2004), hep-ph/0312226.
 - [15] M. Knecht and A. Nyffeler, Phys. Rev. **D65**, 073034 (2002), hep-ph/0111058.
 - [16] E. Bartos, A. Z. Dubnickova, S. Dubnicka, E. A. Kuraev, and E. Zemlyanaya, Nucl. Phys. **B632**, 330 (2002), hep-ph/0106084.
 - [17] A. A. Pivovarov, Phys. Atom. Nucl. **66**, 902 (2003), hep-ph/0110248.
 - [18] M. Hayakawa, T. Blum, T. Izubuchi, and N. Yamada, PoS **LAT2005**, 353 (2006), hep-lat/0509016.
 - [19] I. V. Anikin, A. E. Dorokhov, and L. Tomio, Phys. Part. Nucl. **31**, 509 (2000).
 - [20] A. E. Dorokhov and W. Broniowski, Eur. Phys. J. **C32**, 79 (2003), hep-ph/0305037.
 - [21] J. Callan, Curtis G., R. F. Dashen, and D. J. Gross, Phys. Rev. **D17**, 2717 (1978).
 - [22] E. V. Shuryak, Nucl. Phys. **B203**, 93 (1982).
 - [23] D. Diakonov and V. Y. Petrov, Nucl. Phys. **B272**, 457 (1986).
 - [24] A. E. Dorokhov, Phys. Rev. **D70**, 094011 (2004), hep-ph/0405153.
 - [25] A. E. Dorokhov, JETP Lett. **77**, 63 (2003), hep-ph/0212156.
 - [26] A. E. Dorokhov, Eur. Phys. J. **C42**, 309 (2005), hep-ph/0505007.
 - [27] A. E. Dorokhov, JETP Lett. **82**, 1 (2005), hep-ph/0505196.
 - [28] J. Aldins, T. Kinoshita, S. J. Brodsky, and A. J. Dufner, Phys. Rev. **D1**, 2378 (1970).
 - [29] A. Vainshtein, Phys. Lett. **B569**, 187 (2003), hep-ph/0212231.

- [30] S. V. Mikhailov and A. V. Radyushkin, *Sov. J. Nucl. Phys.* **49**, 494 (1989).
- [31] S. V. Mikhailov and A. V. Radyushkin, *Phys. Rev.* **D45**, 1754 (1992).
- [32] A. E. Dorokhov, S. V. Esaibegian, and S. V. Mikhailov, *Phys. Rev.* **D56**, 4062 (1997), hep-ph/9702417.
- [33] T. Schafer and E. V. Shuryak, *Rev. Mod. Phys.* **70**, 323 (1998), hep-ph/9610451.
- [34] W. Broniowski, (1999), hep-ph/9911204.
- [35] R. S. Plant and M. C. Birse, *Nucl. Phys.* **A628**, 607 (1998), hep-ph/9705372.
- [36] A. E. Dorokhov and L. Tomio, *Phys. Rev.* **D62**, 014016 (2000).
- [37] R. D. Bowler and M. C. Birse, *Nucl. Phys.* **A582**, 655 (1995), hep-ph/9407336.
- [38] J. Gasser and H. Leutwyler, *Ann. Phys.* **158**, 142 (1984).
- [39] G. P. Lepage, *J. Comp. Phys.* **27**, 192 (1978).
- [40] J. Bijnens and J. Prades, *Mod. Phys. Lett.* **A22**, 767 (2007), hep-ph/0702170.
- [41] F. Jegerlehner, talk at Int. Workshop on e+e- collisions from Phi to Psi, www.lnf.infn.it/conference/phipsi08 (7-10 April 2008).
- [42] M. Knecht and A. Nyffeler, *Eur. Phys. J.* **C21**, 659 (2001), hep-ph/0106034.
- [43] P. Maris and C. D. Roberts, *Phys. Rev.* **C58**, 3659 (1998), nucl-th/9804062.
- [44] I. V. Anikin, A. E. Dorokhov, and L. Tomio, *Phys. Lett.* **B475**, 361 (2000), hep-ph/9909368.